Electronic Supplementary Material (ESI) for Dalton Transactions

Supporting Information

Table S1 Crystallographic data for **1** and **3a**

	1	**3a**
formula	$C_{47}H_{36}FeN_6O_2P$	$C_{78}H_{62}F_4Fe_2\ Mn_2N_{16}O_{11}$
formula weight	803.64	848.51
crystal system	triclinic	monoclinic
space group	P-1	$P2_1/n$
temperature (K)	293	293
a (Å)	9.0359(8)	8.8536(15)
b (Å)	15.6389(14)	19.518(4)
c (Å)	15.8476(14)	20.676(4)
α (°)	65.717(3)	90
β (°)	79.311(3)	93.255(5)
γ (°)	79.589(3)	90
V(Å^3)	1992.2(3)	3567.1(11)
Z	2	4
ρ_{calc} (g cm^{-3})	1.340	1.580
μ (mm^{-1})	0.466	0.832
F(000)	834	1736
reflections collected/unique (R_{int})	32420/9445 (0.2668)	28572/8266 (0.3364)
Goodness-of-fit	1.227	1.057
R1[a] [I>2σ(I)]	0.1352	0.1509
wR2[b] [I>2σ(I)]	0.2573	0.3214

$^a R1=\Sigma||F_O|-|F_C||/\Sigma|F_C|$, $^b wR2 = [\Sigma w(F_O^2 - F_C^2)^2/\Sigma w(F_O^2)^2]^{1/2}$

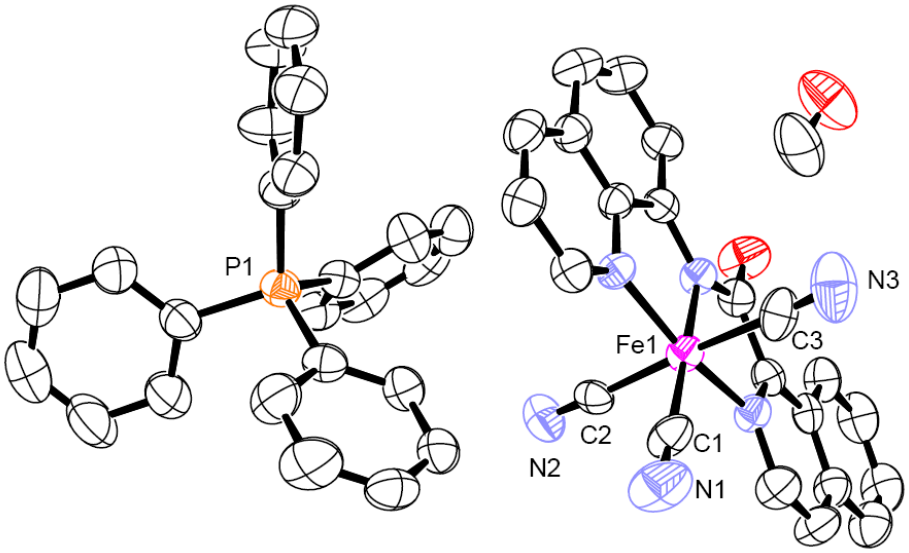

Fig. S1 Crystal structure of **1**.

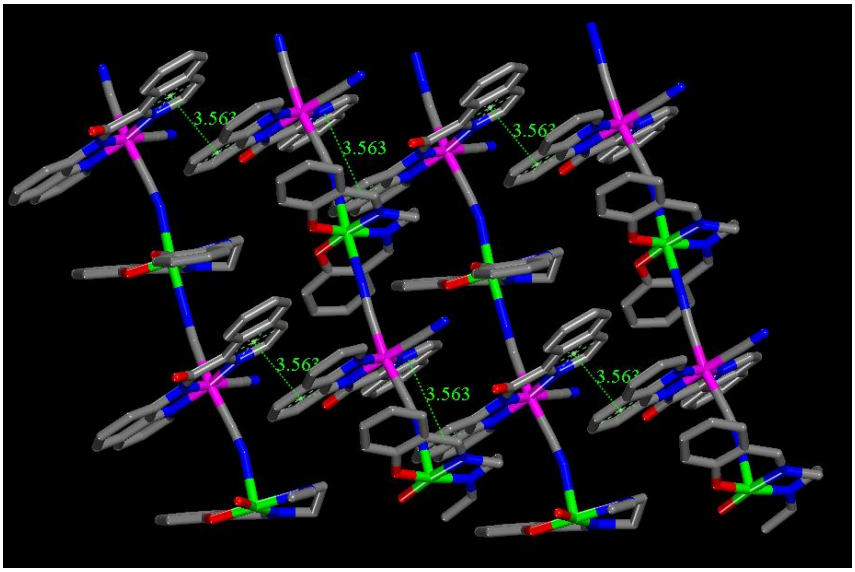

Fig. S2 Extended view of **2** displaying π-π stacking forces between pyridyl and benzene rings of quinoline groups of iqc (centroid distance = 3.563 Å), which affords the formation of a 2D sheet structure.

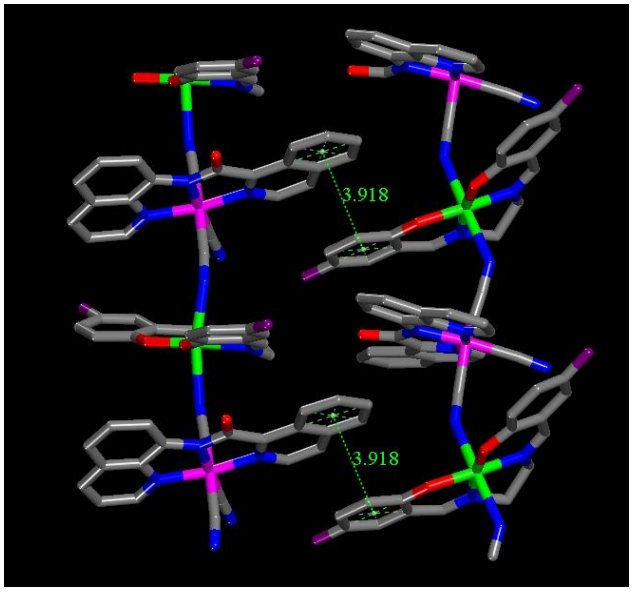

Fig S3 Extended view of **3** displaying π-π stacking forces between phenoxide rings of 5-Fsalen and benzene rings of quinoline groups of iqc (centroid distance = 3.918 Å), which affords the formation of a 2D sheet structure.

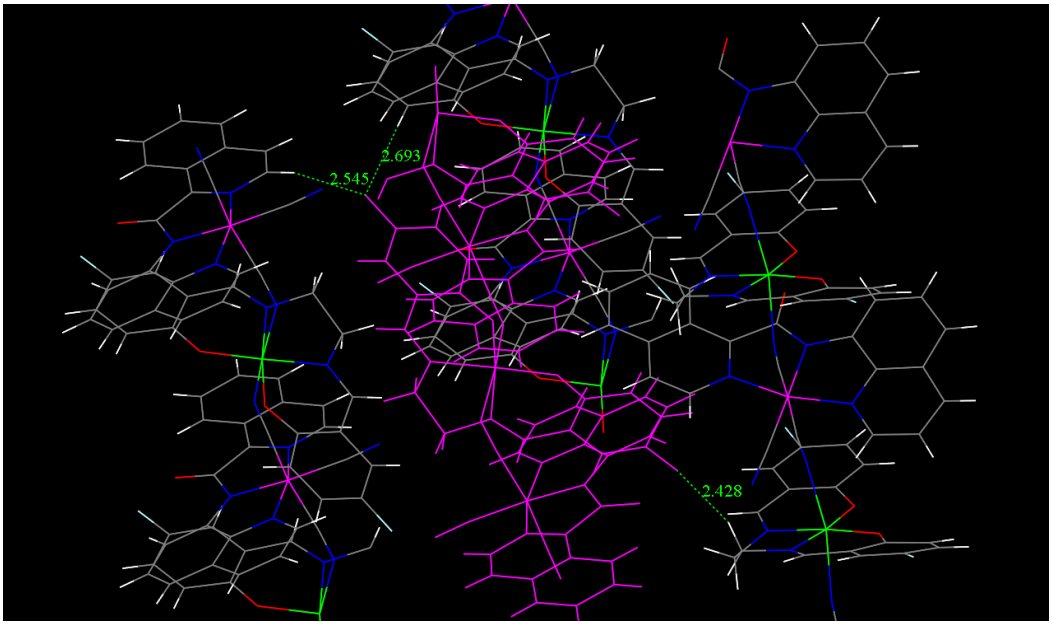

Fig. S4 Crystal packing of **3** showing F---H-C interactions.

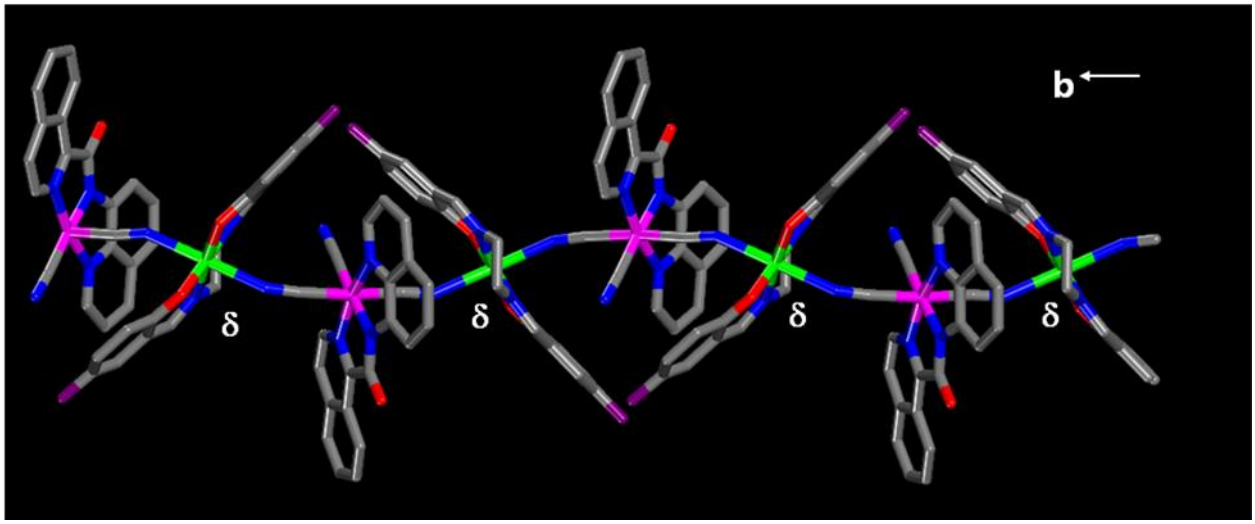

Fig. S5 Enantiomeric chelate-ring conformation of **3a** exhibiting -δ-δ-δ- sequence of chelate rings formed by ethylenediamines, which imparts a P-helical chain.

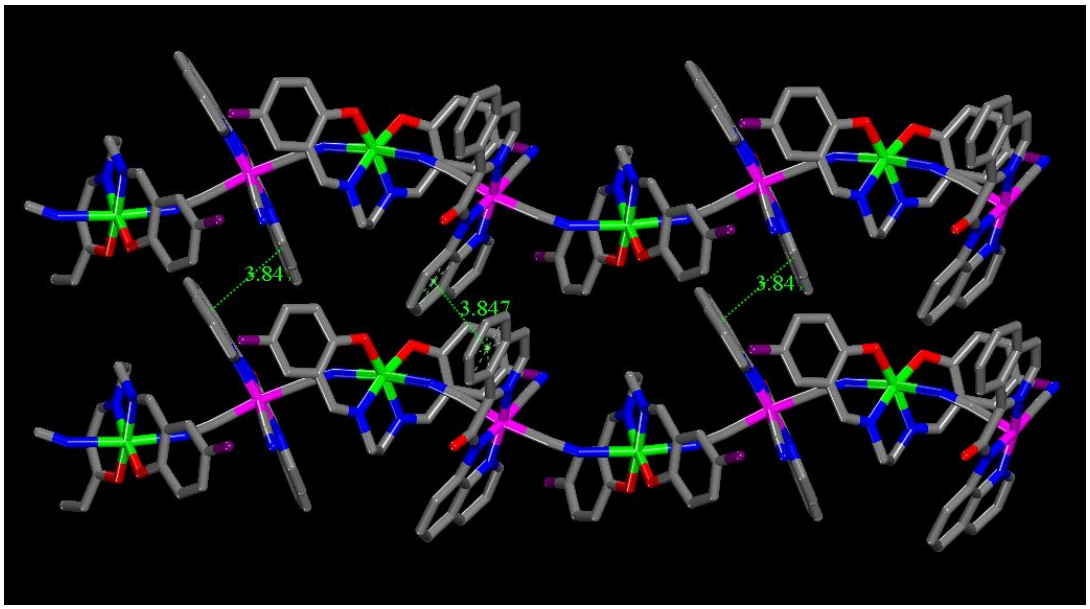

Fig. S6 Extended view of **3a** displaying π-π stacking forces between benzene rings of quinoline and aminoquinoline of iqc ligands (centroid distance = 3.847 Å).

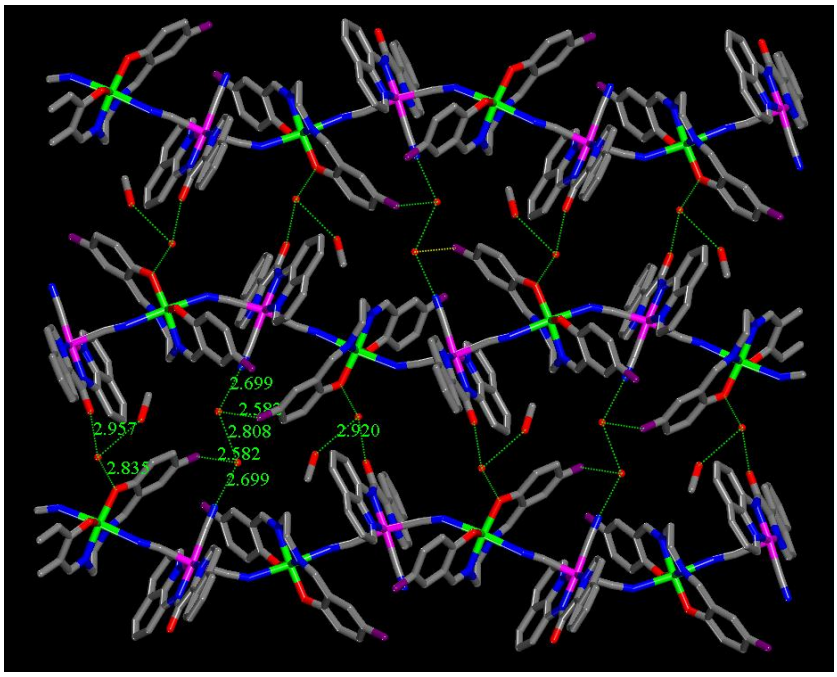

Fig. S7 Extended view of **3a** showing hydrogen bonds among water molecules, MeOH, free CN groups, amide oxygens, and phenoxide oxygens. The F atoms are oriented toward the water molecules. The combination of the hydrogen bonds leads to the construction of a 2D sheet.

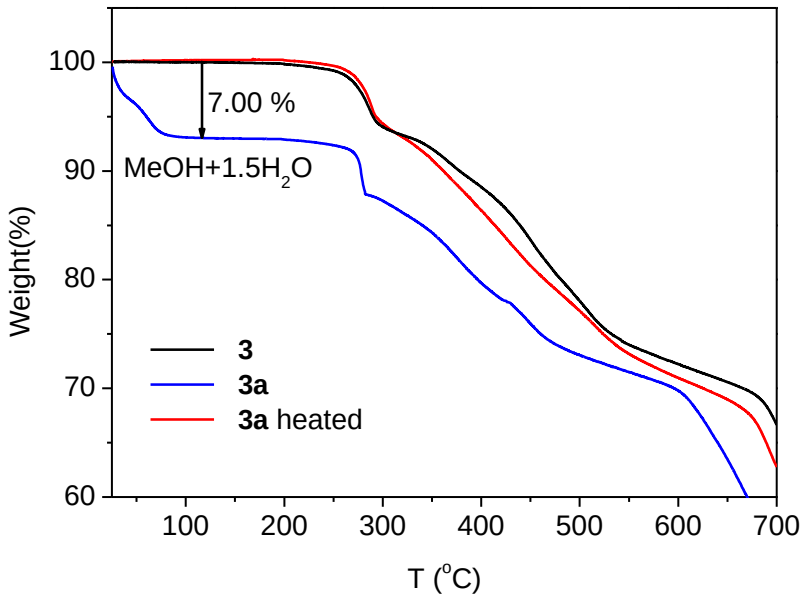

Fig. S8 TGA diagram of **3** and **3a**. The solvents molecules (theoretical weight loss of 7.29 %) were added and removed reversibly.

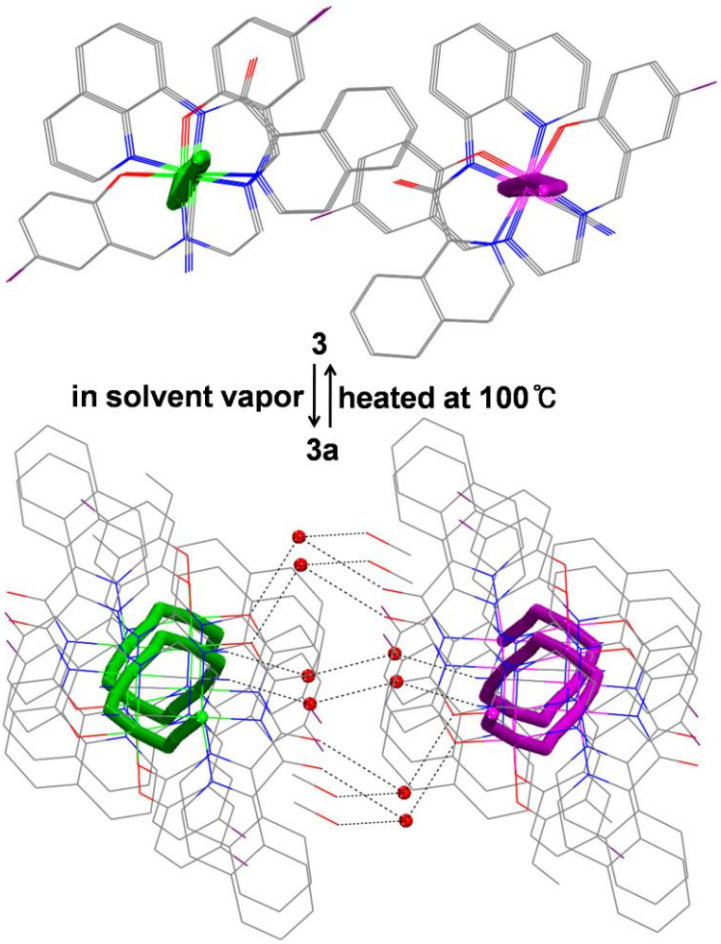

Fig. S9 Structural transformations between **3** and **3a** upon desolvation-solvation protocol. Helical chains with P- (left) and M-helicity (right) for **3a**. The dotted lines represent hydrogen bonds.

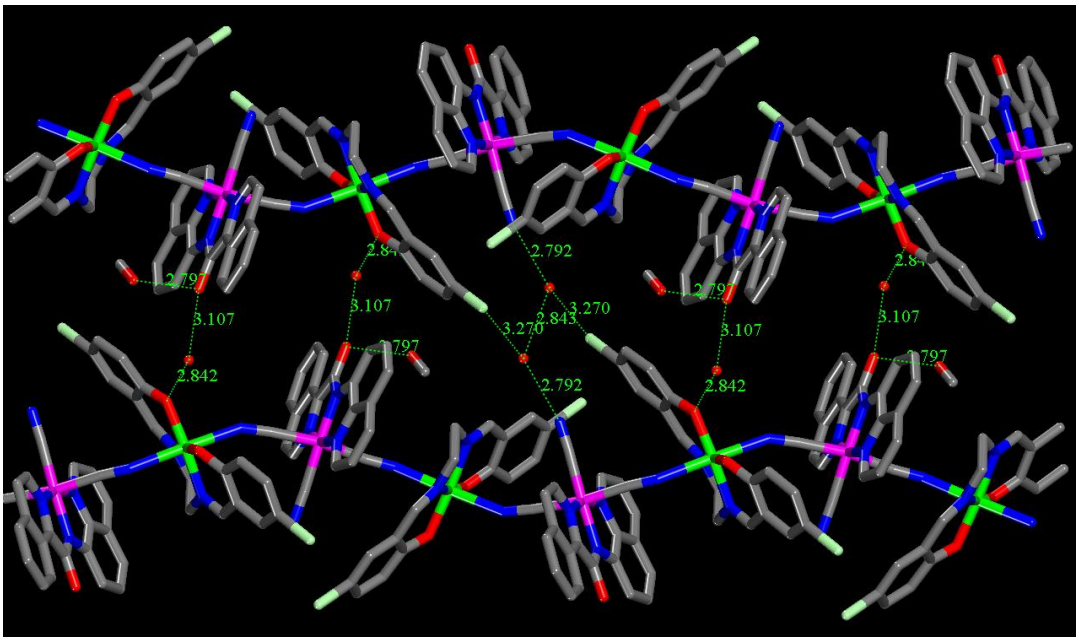

Fig. S10 Extended view of **4** showing hydrogen bonds among water molecules, MeOH, free CN groups, amide oxygens, and phenoxide oxygens. The Cl atoms are oriented toward the water molecules. The combination of the hydrogen bonds leads to the construction of a 2D sheet.

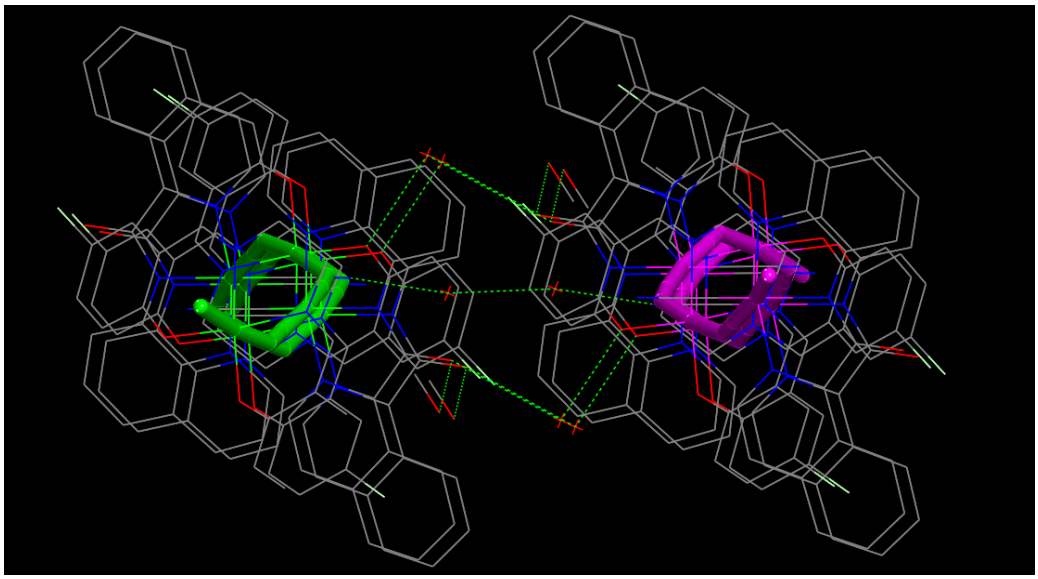

Fig. S11 Helical chains with M- (left) and P-helicity (right) for **4**. The dotted lines denote hydrogen bonds.

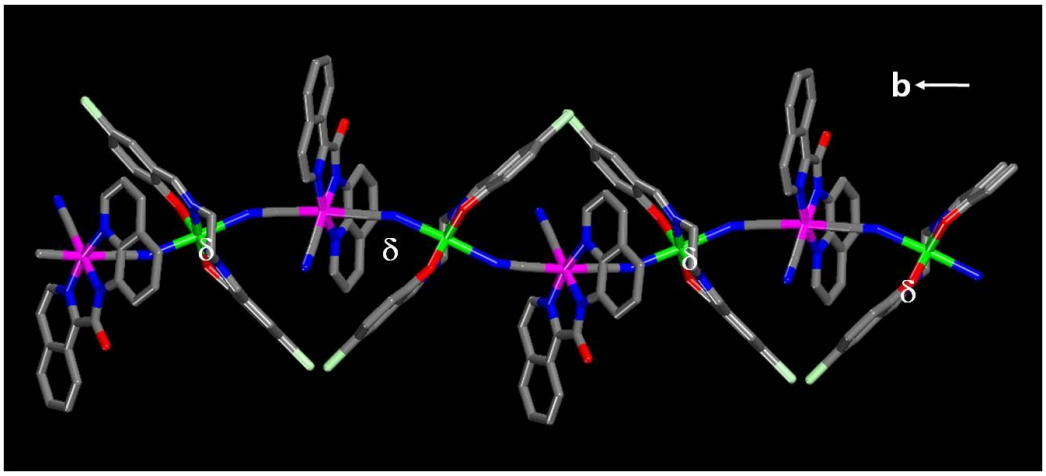

Fig. S12 Enantiomeric chelate-ring conformation of **4** exhibiting -δ-δ-δ- sequence of chelate rings formed by ethylenediamines, which gives a P-helical chain.

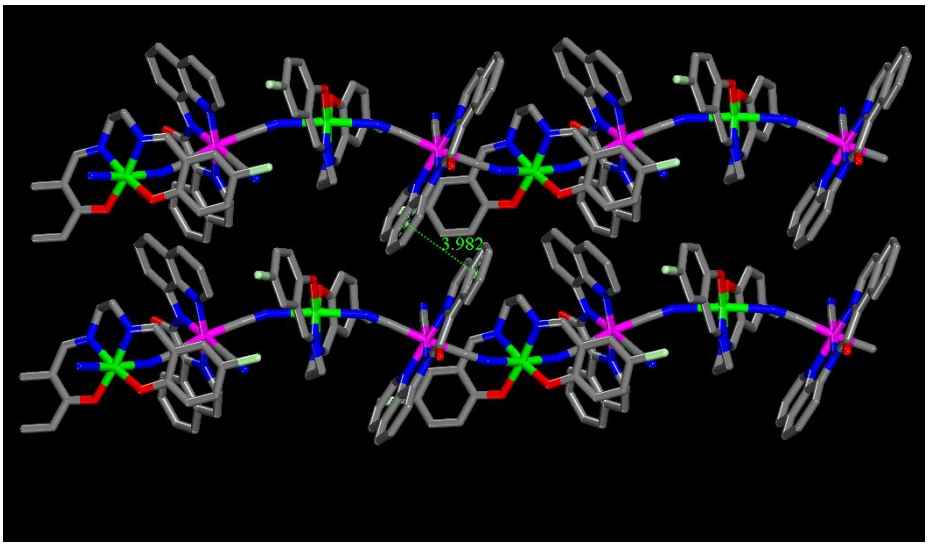

Fig. S13 Extended view of **4** displaying π-π stacking forces between benzene rings of quinoline and aminoquinoline of iqc ligands (centroid distance = 3.982 Å).

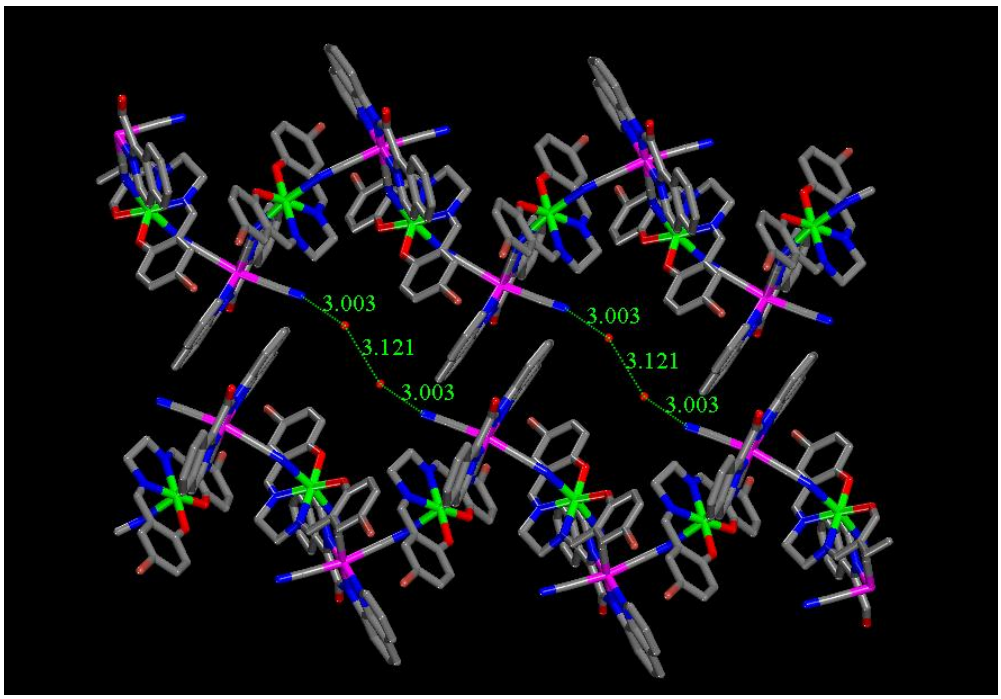

Fig. S14 Extended view of **5** showing hydrogen bonds among water molecules and free CN groups. The combination of the hydrogen bonds leads to the construction of a 2D sheet.

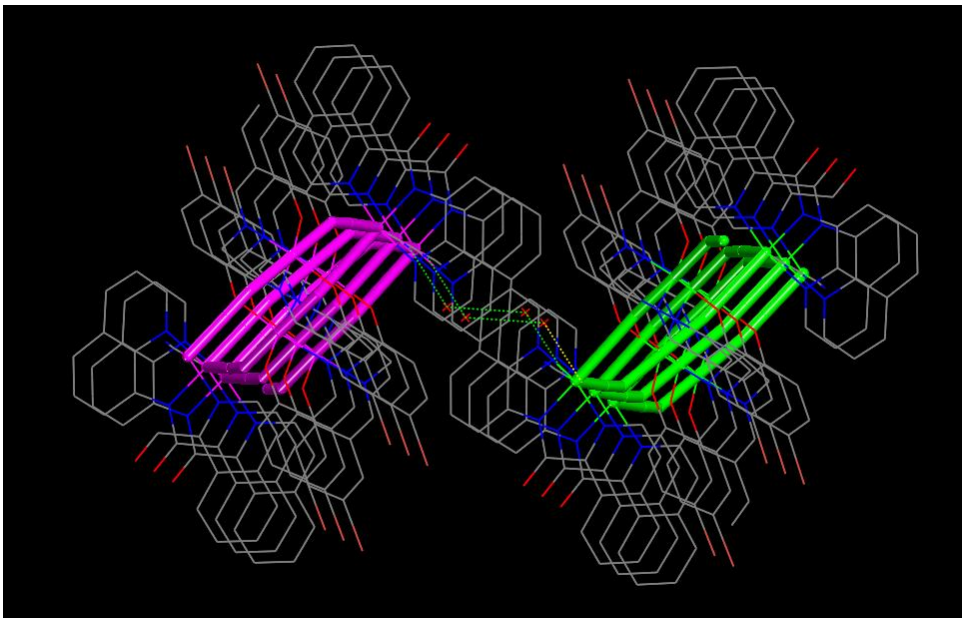

Fig. S15 Helical chains with P- (left) and M-helicity (right) for **5**. The dotted lines denote hydrogen bonds.

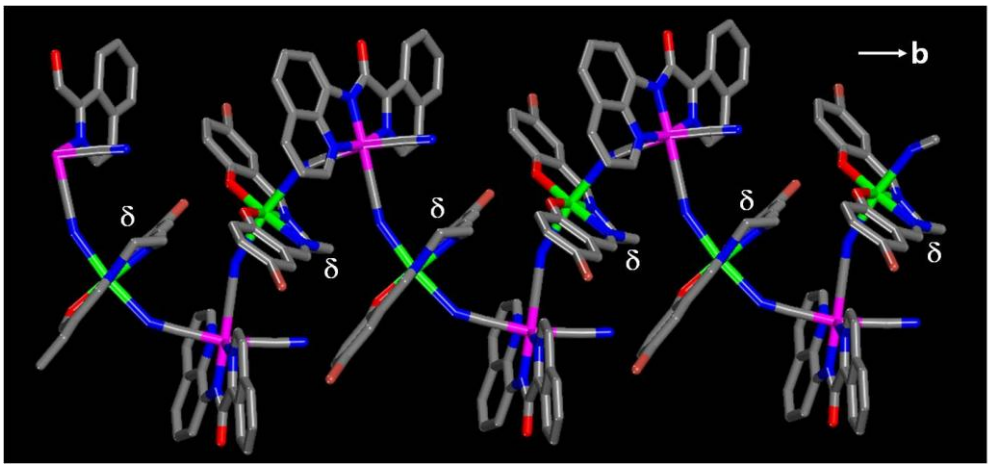

Fig. S16 Enantiomeric chelate-ring conformation of **5** exhibiting -δ-δ-δ- sequence of chelate rings formed by ethylenediamines, which gives a P-helical chain.

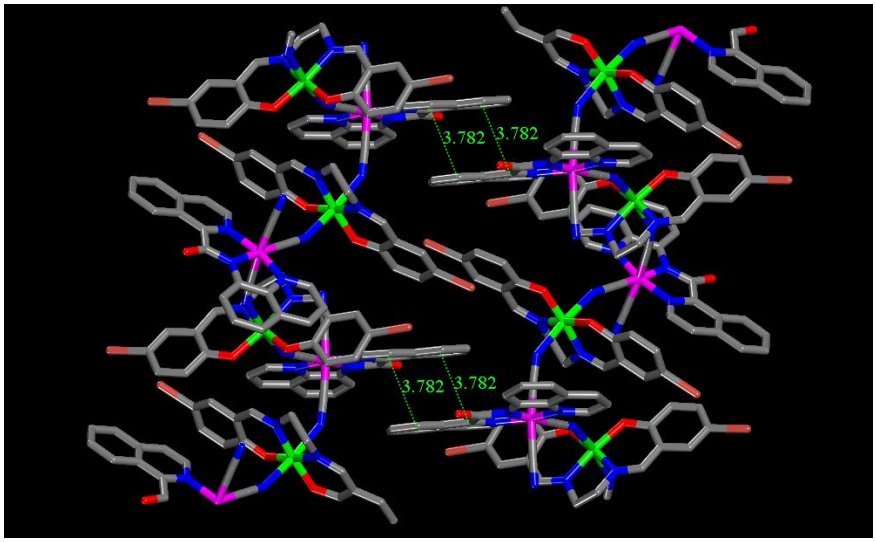

Fig. S17 Extended view of **5** displaying π-π stacking forces between benzene rings of quinoline rings of iqc ligands (centroid distance = 3.782 Å).

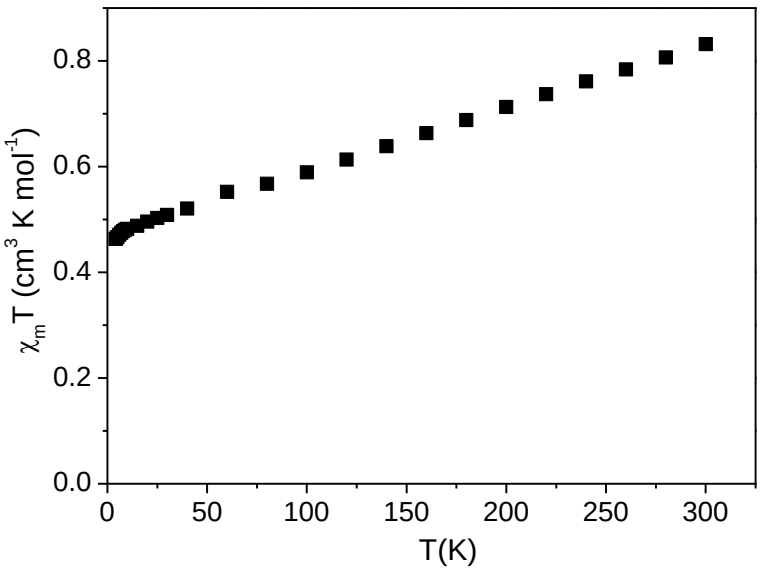

Fig. S18 Plot of $\chi_m T$ versus T of **1**.

The magnetic data of **1** were collected in the temperature range 2-300 K and 1000 G, as depicted in Figure S18. The $\chi_m T$ value is equal to 0.83 cm^3 K mol^{-1} at 300 K, which is much larger than the spin-only value (0.375 cm^3 K mol^{-1}) for a noncoupled $S_{Fe} = 1/2$ but similar to those reported for low-spin Fe(III) analogues.[s1] The $\chi_m T$ behavior on lowering the temperature is due to the presence of an octahedral low-spin Fe(III) ion with the $^2T_{2g}$ ground term and/or temperature-independent paramagnetism.[s1]

(s1) (a) R. Lescouëzec, F. Lloret, M. Julve, J. Vaissermann, M. Verdaguer, R. Llusar, S. Uriel, *Inorg. Chem.*, 2001, **40**, 2065; (b) L. M. Toma, R. Lescouëzec, L. D. Toma, F. Lloret, M. Julve, J. Vaissermann, M. Andruh, *J. Chem. Soc., Dalton Trans.*, 2002, 3171.

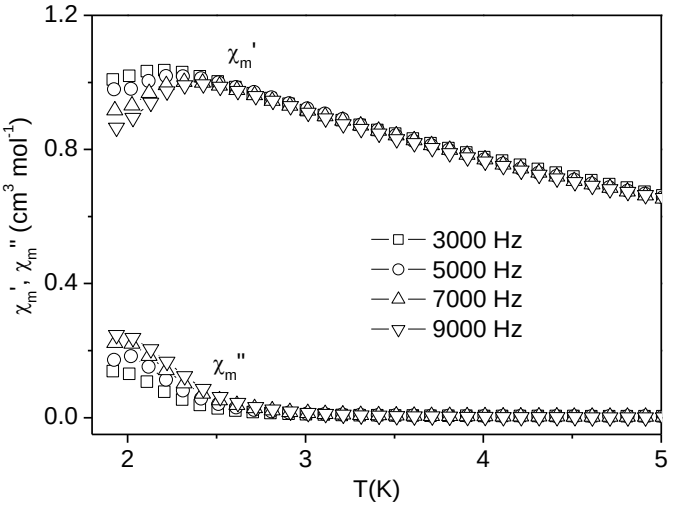

Fig. S19 Plots of in-phase (χ_m') and out-of-phase (χ_m'') signals versus T of **2**.

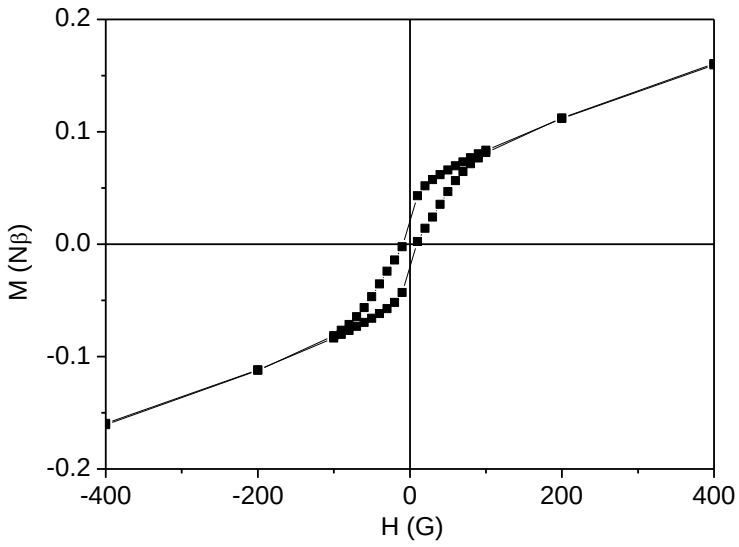

Fig. S20 Blow-up of the magnetization at low fields for **3** at 2 K.

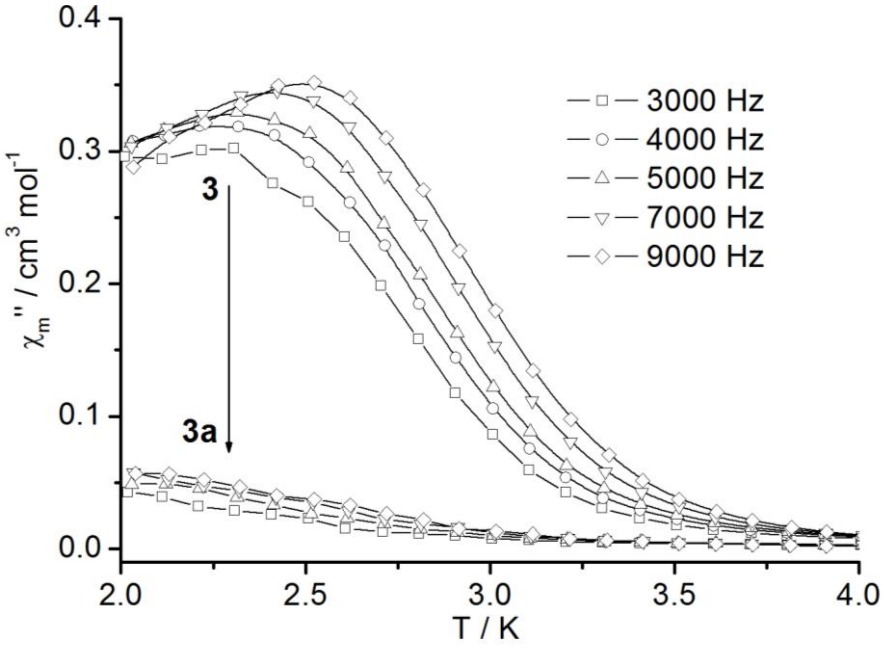

Fig. S21 Out-of-phase ac data at indicated frequencies for **3** and **3a**.

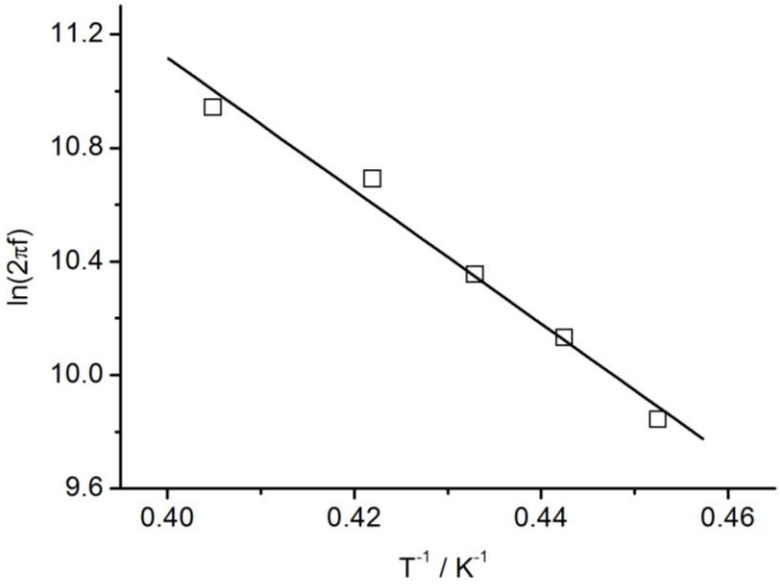

Fig. S22 Arrhenius plot for **3**. The solid line stands for the least-squares fit of maxima in χ_m" to the Arrhenius equation.

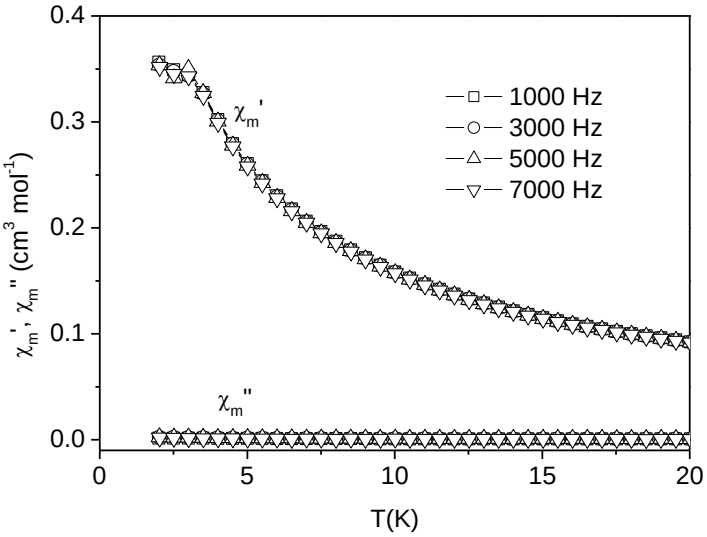

Fig. S23 Plots of χ_m' and χ_m" versus *T* for **4**.

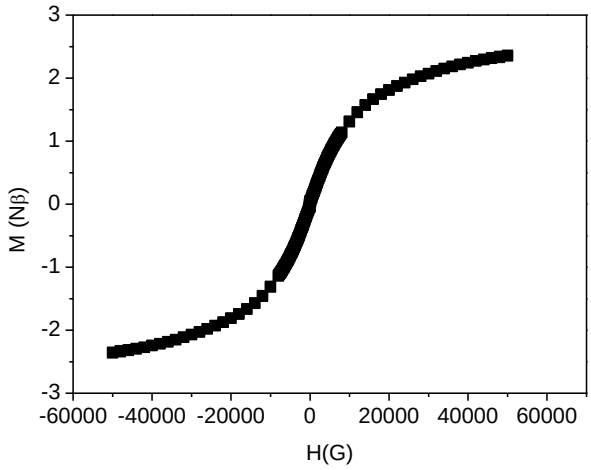

Fig. S24 Plot of *M* versus *H* at 2 K for **5**.

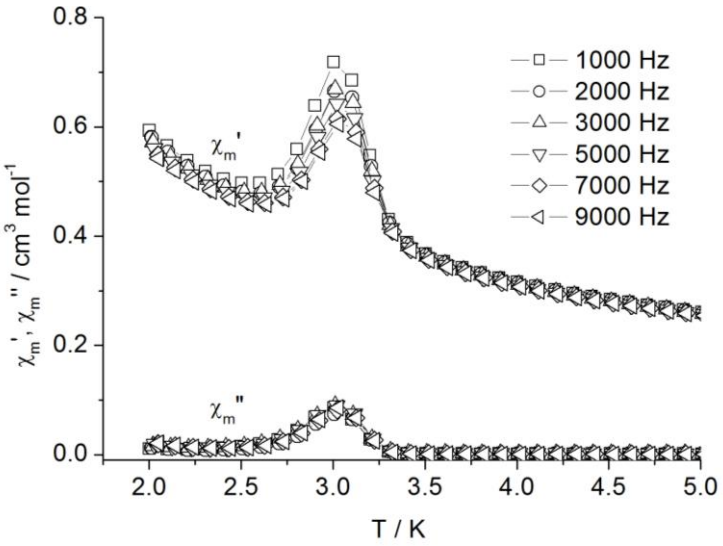

Fig. S25 Plots of χ_m' and χ_m" versus *T* at the indicated frequencies for **5**.

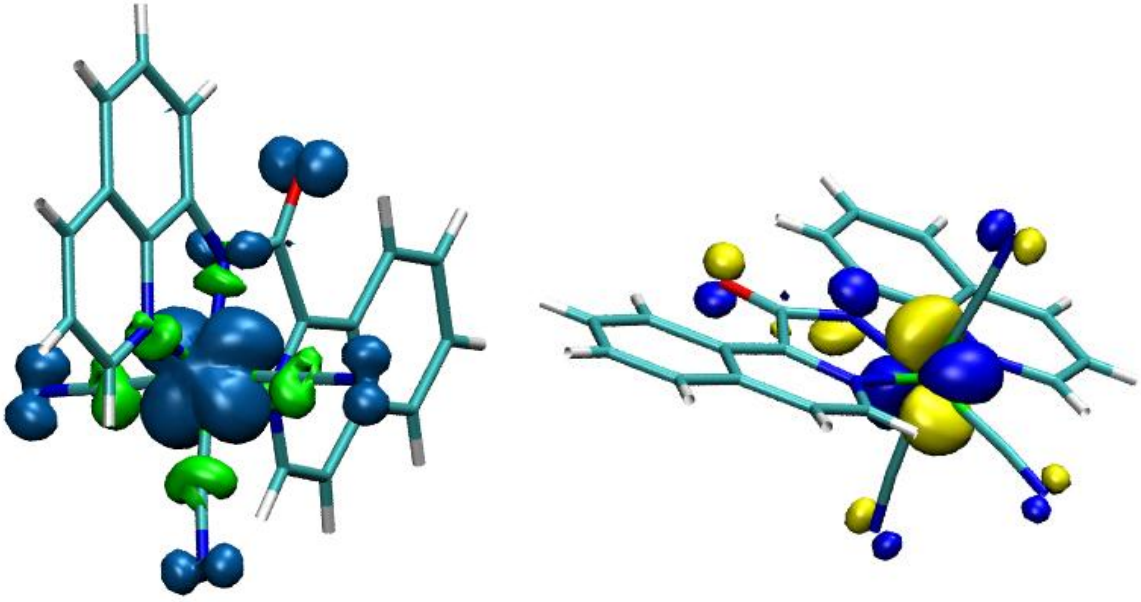

(a) (b)

Fig. S26 a) Spin density of $[Fe(iqc)(CN)_3]^-$ moiety displaying the d_{xz} shape on Fe. The excess α and β spins are shown in blue and green, respectively. The isovalue of the surface is 0.002 e $Å^{-3}$. b) Magnetic natural orbital of the precursor. This result is derived from B3LYP DFT calculations[s1] performed with Gaussian 09. The 6-311G* basis set[s2] is used for the Fe ion and the bound atoms, and the 6-31G basis set[s3] is taken for the other atoms.

(s1) (a) A. D. Becke, *Phys. ReV. A*, 1988, **38**, 3098; (b) C. T. Lee, W. T. Yang, R. G. Parr, *Phys. Rev. B*, 1988, **37**, 785; (c) P. J. Stephens, F. J. Devlin, C. F. Chabalowski, M. J. Frisch, *J. Phys. Chem.*, 1994, **98**, 11623.

(s2) (a) R. Krishnan, J. S. Binkley, R. Seeger, J. A. Pople, *J. Chem. Phys.*, 1980, **72**, 650; (b) A. D. McLean, G. S. Chandler, *J. Chem. Phys.*, 1980, **72**, 5639.

(s3) (a) W. J. Hehre, R. Ditchfield, J. A. Pople, *J. Chem. Phys.*, 1972, **56**, 2257; (b) P. C. Hariharan, J. A. Pople, *Theor. Chim. Acta*, 1973, **28**, 213.